Magnetic Resonance Letters 1 (2021) 99–111

Contents lists available at ScienceDirect

Magnetic Resonance Letters

journal homepage: www.keaipublishing.com/MRL

Perspective

Detecting water-protein chemical exchange in membrane-bound proteins/peptides by solid-state NMR spectroscopy☆

Dedicated to Professor Xiuwen Han on the occasion of her 80th birthday

ARTICLE INFO

Article history:
Available online 30 November 2021

Keywords:
Chemical exchange
Spin diffusion
HETCOR
CEST
Water-protein interactions
Solid-state NMR

ABSTRACT

Water plays an important role in many essential biological processes of membrane proteins in hydrated lipid environments. In general, the ^{1}H polarization transfers between water molecules and site-specific protons in proteins can be classified as coherent (via dipolar spin diffusion) and incoherent (via chemical exchange and nuclear Overhauser effect) transfers. Solid-state NMR is the technique of choice for studying such water-protein interactions in membrane-bound proteins/peptides through the detection of ^{1}H polarization transfers from water to the proteins. These polarization transfer mechanisms often exist simultaneously and are difficult to quantify individually. Here, we review water-protein polarization transfer techniques in solid-state NMR, with a focus on the recent progress for the direct detection of site-specific kinetic water-protein chemical exchange processes on the sub-millisecond time scale in membrane-bound proteins. The measurements of the pure chemical exchange kinetics provide a unique opportunity to understand the role that water plays in the structure-function relationships of membrane-bound species at the water-bilayer interface. In addition, the perspective of chemical exchange saturation transfer (CEST) experiments in membrane-bound proteins/peptides is further discussed.

1. Introduction

Biological membranes are comprised of crowded membrane-bound proteins in a hydrated lipid environment [1]. These proteins conduct many essential biological processes with the aid of water, such as inter- and intra-cellular signal transduction across complex cellular and organelle membranes [2–4]. The membrane lipid interactions are well studied and have profound impacts on the structure and function of membrane-bound proteins and peptides [5–9]. However, water-protein interactions [10–15] are also critically important for understanding how proteins function in their complex environment. Nuclear magnetic resonance (NMR) is the only spectroscopic technique with atomic resolution that is capable of studying water-protein interactions in detail. In solution NMR, water-protein interactions have been intensively used to study protein dynamics and binding via relaxation parameters using multi-dimensional NMR [16–19]. On the other hand, a growing number of solid-state NMR studies of water-protein interactions using magic-angle-spinning (MAS) [15,20–28] and oriented samples [29] have been reported. These studies have demonstrated that the water-protein interactions can be revealed through ^{1}H-^{1}H polarization transfer between water and specific proton sites in proteins, mediated by coherent ^{1}H dipolar spin diffusion (SD) and incoherent chemical exchange or nuclear Overhauser effect (NOE) [25,30,31]. Chemical exchange is the proton substitution process between the proton in water molecules and the exchangeable protons in the proteins. SD is the distance-dependent magnetization transfer through ^{1}H-^{1}H dipolar interactions and is considered to be the most efficient ^{1}H-^{1}H polarization transfer mechanism in the presence of strong proton dipolar interactions, such as in rigid solids. The NOE is based on dipolar cross effects between two motional-modulated spins that are in close proximity. These polarization transfer mechanisms provide an opportunity for characterizing how the protein interacts with water. For instance, H/D

☆ Peer review under the responsibility of Innovation Academy for Precision Measurement Science and Technology (APM), CAS.

https://doi.org/10.1016/j.mrl.2021.09.002
2772-5162

Abbreviations

CEST	chemical exchange saturation transfer
CP	cross polarization
DOPC	1,2-dioleoyl-*sn*-glycero-3-phosphocholine
DOPE	1,2-dioleoyl-*sn*-glycero-3-phosphoethanolamine
DMPC	dimyristoylphosphatidylcholine
gA	gramicidin A
HETCOR	heteronuclear correlation
LG	Lee-Goldburg
LGCP	Lee-Goldburg cross polarization
LGSL	Lee-Goldburg spin-lock
M2FL	full length M2
MA	magic angle
MAS	magic-angle-spinning
NMR	nuclear magnetic resonance
NOE	nuclear Overhauser effect
REDOR	rotational-echo double-resonance
SD	spin diffusion
TM	transmembrane

exchange experiments allow one to characterize the accessibility of water in the M2 proton channel of the Influenza A virus [32] to the transmembrane helical backbone and how the deuterated water participates in conformational changes in proteins [33]. Moreover, SD experiments can effectively identify those residues that are exposed to water, such as forming hydrogen-bonds with water [34]. However, these mechanisms are often present simultaneously in water-protein polarization transfer experiments [31]. Especially in the presence of strong ^{1}H intramolecular SD associated with the relatively rigid membrane-bound protein environments and because of the very high concentration of water surrounding the membranes, observing site-specific chemical exchange between water molecules and specific proton sites in a protein is rather difficult. In this perspective review, we discuss the water-protein polarization transfer techniques in solid-state NMR, with a focus on the recent progress for detecting site-specific kinetic water-protein chemical exchange processes on the sub-millisecond time scale in membrane-bound proteins/peptides.

As diagramed in Fig. 1, detecting the water-protein chemical exchange in biological solids is different from detecting that in mobile systems. In solution, due to the fast molecular tumbling, the proton dipolar interactions are averaged out. Thus the water-protein interactions are primarily under a chemical exchange process that can be detected through relaxation NMR using multi-dimensional spectroscopy [16–19]. On the other hand, in biological solids, a proton from a protein (colored as red in Fig. 1b) is not only in chemical exchange with water, but also under fast intramolecular dipolar SD with other protons within the protein. When the proton-proton dipolar interactions are very strong, the SD becomes so dominant that any red proton magnetization induced by chemical exchange with water can disperse into other protons in the protein rather quickly, making it difficult to detect the site-specific water-protein chemical exchange. In addition, the protons in those residues that are hydrogen-bonded with water [34] are, in fact, in close proximity with water and thus are subject to the intermolecular dipolar coupling mediated SD polarization transfer from water. Consequently, the observed water-proton polarization transfer could be induced either by chemical exchange or by intermolecular dipolar coupling mediated SD or are simply the result of the relayed polarization transfer, first via chemical exchange and then by the intramolecular dipolar SD, which would lead to very different interpretations of how water interacts with the protein. Here, we will first overview the solid-state NMR techniques for studying water-protein interactions, followed by introducing the recent development for probing pure water-protein chemical exchange in membrane-bound proteins/peptides. Finally, we use the Influenza A full length M2 (M2FL) protein as an example to characterize the M2 proton channel conduction mechanism using the water-protein chemical exchange processes.

2. Solid-state NMR techniques for water-protein polarization transfers

In many two-dimensional (2D) ^{1}H-^{15}N/^{13}C heteronuclear correlation (HETCOR) spectra of membrane-bound proteins/peptides, additional cross-peaks with water protons were clearly observed in both MAS [14,21,27,30,31] and oriented sample [11,29] solid-state NMR. Since a direct polarization from mobile water to proteins is rare (unless the water is confined) [35–37], such cross-peaks with the water protons are believed to take place during the cross polarization (CP) step, which is used for transferring ^{1}H magnetization to ^{15}N/^{13}C spins [21]. In solid-state NMR water-protein interactions in membrane-bound proteins/peptides are studied via the polarization transfer from water to the proteins. A ^{1}H T_2 filter with a

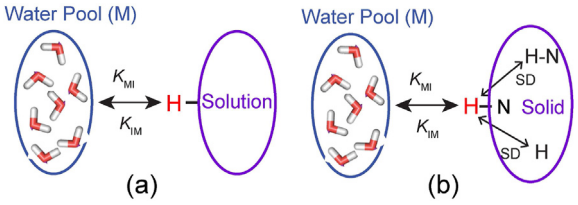

Fig. 1. Schematics for the water-protein chemical exchange processes in solution (a) and in biological solids (b), where K_{IM} and K_{MI} represent the exchange rate constants between the water pool (M) and a specific proton (I) in a protein. Note that in solution the polarization can be further transferred through NOE inside the protein.

sufficiently long echo time τ, as shown in Fig. 2a, largely suppresses all protons in a protein while sufficiently retaining the polarization of the mobile water, so that the mobile water polarization can be spin-locked for polarization transfer to $^{15}N/^{13}C$ sites for one-dimensional (1D) observation via CP. As first demonstrated by Harbison et al. [38], such a ^{1}H T_2 filter allowed for monitoring the kinetic transfer from solvent water to the Schiff-base nitrogen of the bacteriorhodopsin membrane protein. Many sophisticated pulse sequences [20–23,25], including shaped pulses for selectively polarizing the water signals, rotational-echo double-resonance (REDOR)-based dephasing for a ^{1}H T_2 filter, and proton detection versions for improved sensitivity, have been proposed for probing the water-protein interactions. Depending on how the mobile water propagates its polarization to the protons in the protein, two classes of representative schemes are shown in Fig. 2.

First, the mobile water is spin-locked for polarization transfer. Such an 1D version (Fig. 2a) can be extended to 2D homonuclear correlation experiments, as shown in Fig. 2b, allowing for site-specific monitoring of water-protein interactions in complex protein systems [21,31]. It is worthy to note that when the mobile water is spin-locked during the CP contact time, there is, in fact, a mix of coherent dipolar SD (both inter- and intra-molecular dipolar couplings) and incoherent chemical exchange driven contributions. Even with spin-locking the ^{1}H magnetization along the magic-angle (MA) using the Lee-Goldburg (LG) sequence [39] to suppress the dipolar SD, the polarization transfer processes during CP are rather complicated, involving a three-spin system (water proton, a specific proton in the protein, and a $^{15}N/^{13}C$ spin), from which it is not straightforward to extract chemical exchange rates from the spin dynamics [40].

Secondly, the selective polarization of the mobile water is flipped to the z axis for a mixing time, t_{mix}, during which its polarization is transferred to other protons in a protein, as shown in Fig. 2c and d. Again, when the mobile water signal evolves in the indirect dimension t_1, as in Fig. 2d, this allows for site specific monitoring of the transferred polarization buildups. During t_{mix}, the water-protein polarization transfer could be driven by the coherent process via the intermolecular dipolar SD between water and protein when there exists any water-protein hydrogen-bonding, and by the incoherent process through chemical exchange and NOE. As the coherent dipolar SD is primarily dependent upon the dipolar couplings involved, it can be manipulated by experimental techniques. For instance, ^{13}C-^{13}C spin diffusion can be greatly enhanced by the rotary resonance conditions [41–43] during t_{mix} under MAS, and consequently becomes one of the most powerful tools for obtaining ^{13}C-^{13}C homonuclear correlation spectra for protein structural elucidation, but it can also be suppressed by efficient heteronuclear decoupling during the mixing time, such that the chemical exchanged cross peaks can be revealed in the ^{13}C-^{13}C homonuclear correlation spectra [27]. Similarly, when ^{1}H-^{1}H dipolar couplings are suppressed by MAS, the radio frequency-driven recoupling [44] can be used to re-introduce the coherent dipolar SD during t_{mix} [45–47] for the determination of structure and dynamics of membrane-associated peptides. By comparison, the incoherent chemical exchange and NOE represent kinetic processes in the systems and can only be manipulated by temperature, not by any experimental techniques. For the incoherent process, differentiating the chemical exchange and NOE is rather difficult. It is generally believed that NOE between water and protein protons is dominated by long-range dipolar couplings to bulk water [48]. It is worthy to note that, in the presence of strong intramolecular ^{1}H-^{1}H dipolar couplings in the protein, any ^{1}H signal in the protein obtained via the water-protein polarization transfer could be rapidly dispersed into other protons through the intramolecular SD during t_{mix}, such that the detection of the site-specific water-protein transfer is obscured.

3. Water-protein chemical exchange polarization transfer

For relatively rigid membrane-bound proteins/peptides, the intramolecular dipolar SD is the major mechanism for transferring polarization among protons within a protein, as illustrated in Fig. 1b, meaning that any polarization changes of a specific proton induced by a water-protein polarization transfer would be quickly dispersed to other protons that are not subject to direct water-protein interactions. In order to probe site-specific water-protein chemical exchange, minimizing the intramolecular dipolar SD is critically important. In this regard, fast MAS (60 kHz or higher) [49,50], along with diluting the ^{1}H coupling network via protein deuteration, is a convenient way to suppress the strong ^{1}H dipolar interactions for reducing the SD. This can be easily incorporated into NMR techniques shown in Fig. 2 with direct proton detection. Conversely, when the sample is spinning moderately or even under static condition, spin-locking the ^{1}H magnetization along the MA using the LG sequence [39] is an effective way to suppress ^{1}H-^{1}H intramolecular dipolar SD. However, even when the ^{1}H is spin-locked along the MA by the LG sequence during CP (i.e., LGCP), the polarization transfer process from water to protein during

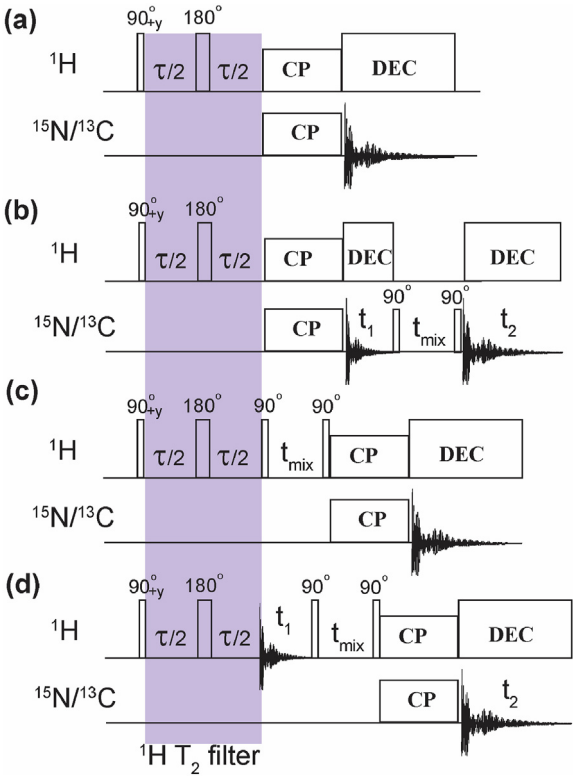

Fig. 2. Representative pulse sequences used for the water-protein polarization transfer with the observation of $^{15}N/^{13}C$ signals via CP. A ^{1}H T_2 filter is highlighted in the beginning of the sequences to suppress the proton signals from the proteins while sufficiently retaining the polarization of the mobile water. The selected water polarization is spin-locked for CP transfer to $^{15}N/^{13}C$ for (a) 1D and (b) 2D observations, or it is flipped to the z axis, (c) without and (d) with its chemical shift evolution, for a period of time t_{mix} allowing for polarization transfer to other protons, followed by detecting $^{15}N/^{13}C$ via CP.

LGCP involves a three-spin system (i.e., water proton, a specific proton in the protein, and a$^{15}N/^{13}C$ spin), making it difficult to extract the water-protein chemical exchange from water to the proton in proteins, as alluded to before [40].

Recently, 1D chemical exchange measurements [15] were proposed, as diagramed in Fig. 3a, to probe specific water-protein chemical exchange kinetics without the influence of SD. Here, the specific proton in a protein is indirectly monitored by its near-by ^{15}N. The specific proton is first dephased by the ^{1}H T_2 filter and then re-polarized via chemical exchange with the mobile water during the Lee-Goldburg spin-lock (LGSL) time (t_{SL}). The main difference, as compared to the schemes in Fig. 2, is that after the ^{1}H T_2 filter the mobile water magnetization remains along the MA in the entire period of the water-protein polarization transfer, such that the SD is minimized. Importantly, only water protons and a specific proton in the protein are involved in polarization transfer during t_{SL}, so that a two-spin system (M—water; I—the specific proton in the protein) can be used to describe the chemical exchange between the M and I spins using the Solomon equations, rather than a complex three-spin system during LGCP:

$$\frac{d\,M(t_{SL})}{d\,t_{SL}} = -\left(\frac{1}{T_{1\rho}^{M}} + K_{MI}\right)M(t_{SL}) + K_{IM}I(t_{SL}) \tag{1}$$

$$\frac{d\,I(t_{SL})}{d\,t_{SL}} = K_{MI}M(t_{SL}) - \left(\frac{1}{T_{1\rho}^{I}} + K_{IM}\right)I(t_{SL}) \tag{2}$$

here $M(t_{SL})$ and $I(t_{SL})$ are the M and I magnetizations along the MA at a given LGSL time, t_{SL}. $T_{1\rho}^{M}$ and $T_{1\rho}^{I}$ are the spin-lattice relaxation times in the LGSL for M and I protons, respectively. Because the M and I magnetizations are along the MA, the cross relaxation between M and I has been negligible in the above equations. p is the concentration of the water molecules in the pool of water M that participate in exchange with the specific proton in the protein. K_{IM} represents the exchange rate constant from the specific I proton to the water molecules, while the exchange rate constant K_{MI} from waters to the specific I proton is p^{*} K_{IM}.

For simplicity, by assuming that the M and I protons have the same spin-lattice relaxation time in the LGSL, i.e., $T_{1\rho}^{M} = T_{1\rho}^{I} = T_{1\rho}^{H}$, the analytical solution can be derived from the Solomon equations [15]:

$$I(t_{SL}) = I(0) + [pM(0) - I(0)]\{1 - \exp[1 - (p+1)K_{IM}t_{SL}]\}\exp\left(-t_{SL} \Big/ T_{1\rho}^{H}\right) \Big/ (p+1) \quad (3)$$

Clearly, the chemical exchange term is scaled by the population difference between the water molecules and the specific proton in the protein involved in the chemical exchange. In the case of one water molecule exchanging with one proton in the protein, the population difference should be null and thus no chemical exchange can be observed during LGSL. Therefore, the trajectory of $I(t_{SL})$ in Eq. (3) is not sensitive to their exchange process. Note that when $I(0)$ represents any residual magnetization due to incomplete dephasing, this residual magnetization will contribute to initial signals, but will not be involved in the chemical exchange process.

On the other hand, when the magnetization $I(0)$ is dephased completely before the LGSL, the solution for $I(t_{SL})$ becomes:

$$I(t_{SL}) = pM(0)\{1 - \exp[-(p+1)K_{IM}t_{SL})]\}\exp\left(-t_{SL} \Big/ T_{1\rho}^{H}\right) \Big/ (p+1) \quad (4)$$

Clearly, the observation of the chemical exchange term in Eq. (4) is now dependent solely on the population of the water molecules that participate in the exchange and builds up the $I(t_{SL})$ magnetization that has been selectively dephased at the beginning of LGSL. Fig. 3b shows the simulated recoveries of the dipolar-dephased ^{1}H magnetization at various chemical exchange rate constants.

Due to the strong ^{1}H spin diffusion associated with the membrane-bound biological systems, in the study of water-protein interactions using the schemes in Fig. 2, all proton magnetization from the protein needs to be dephased during the ^{1}H T_2 filter in order to prevent any ^{1}H-^{1}H SD among protons in the protein from interfering with the specific proton in exchange with the mobile water [24,51]. Often, this requires the ^{1}H T_2 filter to have a long enough echo time τ or simultaneously apply both ^{13}C and ^{15}N REDOR dephasings for a long period of time when there exist relatively mobile functional groups, such as methyl and ammonium groups, to suppress all protons in the protein. In contrast, in the scheme shown in Fig. 3a, the ^{1}H magnetization is spin-locked along the MA [39] where the ^{1}H-^{1}H SD is suppressed, thus no ^{1}H-^{1}H polarization transfer among the protein protons is expected. Therefore, it is sufficient to dephase only the ^{1}H magnetization that is bonded with the indirectly observed ^{15}N site. Fig. 4 shows the spectra in control experiments using an amino acid histidine powder sample lyophilized from a pH 6.3 solution. At this given pH, the histidine exists in two tautomeric states [52], i.e., the neutral τ and charged states (shown in the insert of Fig. 4a). When the ^{15}N 180° pulses were not applied (i.e., without REDOR), all three protonated nitrogen sites ($N^{\tau}_{\varepsilon 2}$, $N^{+}_{\delta 1}$, and $N^{+}_{\varepsilon 2}$) were observed, while the non-protonated $N^{\tau}_{\delta 1}$ was not observable because of the short LGCP contact time used in the experiments. When the 180° pulses were applied on ^{15}N (i.e., with REDOR), the intensities for those protonated nitrogen sites ($N^{\tau}_{\varepsilon 2}$, $N^{+}_{\delta 1}$, and $N^{+}_{\varepsilon 2}$) were dramatically decreased, indicating that the dephasing is sufficient with 154 μs dephasing time for the directly bonded NH pairs (having a dipolar coupling of ~10 kHz) [53].

The protons directly bonded with the aromatic nitrogen are effectively dephased by ^{15}N REDOR, but other protons such as C_α-, C_β-, and aromatic ring carbon protons remain. The big question is whether or not those protons would be transferred to the ^{15}N dephased proton through SD during LGSL? Fig. 4b shows the dipolar-dephased ^{15}N MAS NMR spectra of the histidine powder lyophilized from a pH 6.3 solution at different t_{SL}. Clearly, the REDOR-dephased protonated ^{15}N resonances do not gain intensity as t_{SL} increases, implying that the protons that are covalently bonded with the nitrogen do not gain any magnetization from other protons through SD. In fact, there is a slight decrease in intensities due to the proton spin-lattice relaxation time along the MA.

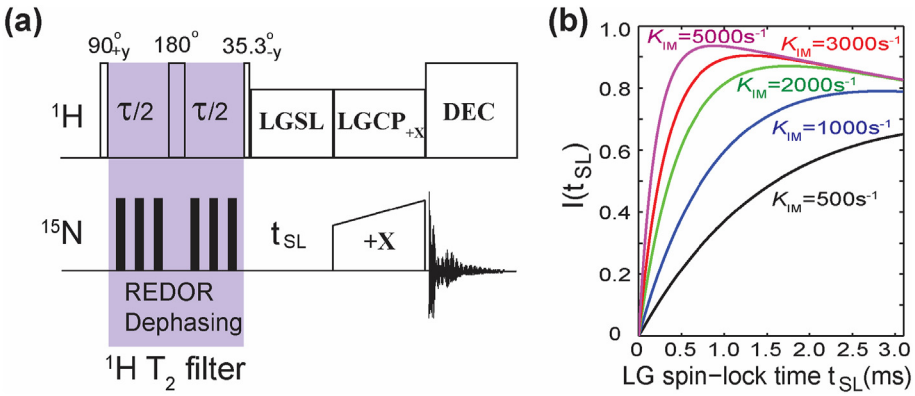

Fig. 3. (a) 1D pulse sequence used to probe water-protein chemical exchange indirectly via ^{15}N. (b) Simulated buildups of the dipolar-dephased ^{1}H magnetization as a function of spin-lock time t_{SL} at various exchange rate constants. Adapted with permission from Ref. [15] Copyright 2021 American Chemical Society.

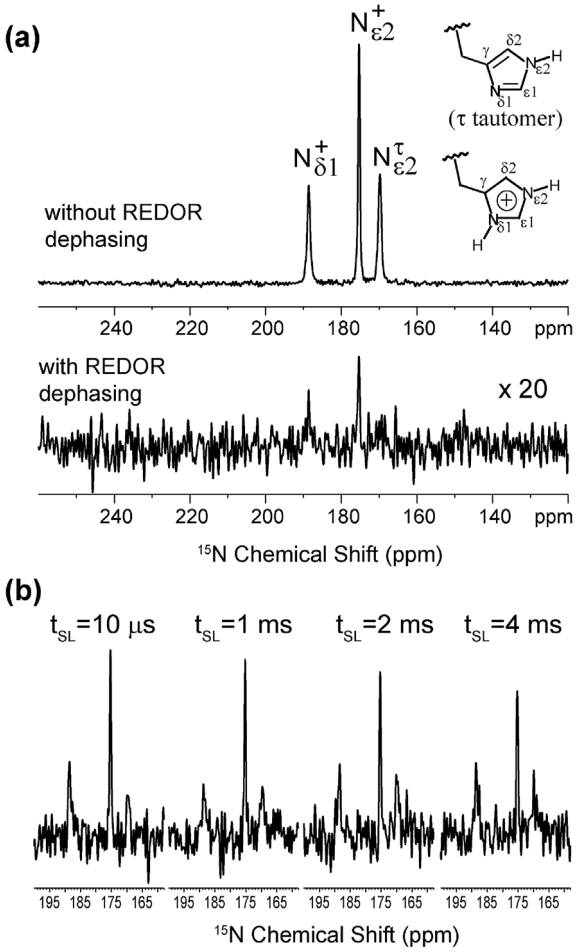

Fig. 4. (a) ^{15}N MAS NMR spectra in the aromatic region of the histidine powder lyophilized from a pH 6.3 solution with and without ^{15}N dipolar dephasing at t_{SL}= 100 μs using the pulse sequence in Fig. 3a. 256 scans were used for signal averaging. (b) Dipolar-dephased ^{15}N MAS NMR spectra in the aromatic region at different t_{SL}. 2048 scans were used for signal averaging. In these experiments, the LGCP contact time of 200 μs and a total dephasing time of two rotor periods, i.e., 154 μs, were used.

4. Characterization of the M2 proton conduction mechanism using the water-protein chemical exchange processes

The M2 protein from the Influenza A virus is a 97-residue membrane protein with a 24-residue N-terminus and a 51-residue C-terminal segment connected by a single transmembrane (TM) helix of 22 residues. It assembles as a tetrameric bundle that conducts protons at a slow rate (10^2-10^3/s) when activated at low pH, which is essential for the viral life cycle [54,55]. The α-helical TM domain (residues 25–46) is responsible for proton conductance triggering the release of viral RNA into the host cells. This tetrameric TM domain is an important drug target [56–59]. Fig. 5a shows the conductance domain of the M2 proton channel, where the four His_{37} residues residing just below the center of the TM helix are known as the heart of the proton conducting channel, the key to the mechanism of proton transport [10]. There have been two debated proton transport mechanisms in the literature: 1) the low-barrier hydrogen bond model in which the proton is transferred through the breaking and reforming of hydrogen-bonds between two pairs of His_{37} dimers [10,60] or 2) the proton shuttling model in which an individual His_{37} residue shuttles protons through imidazole ring reorientations and exchanges protons with water without the process of forming inter-monomer His_{37} hydrogen-bonds [12,13]. Although M2 spectra dramatically vary depending on the M2 constructs and lipids used in sample preparation [12,61–66], the ^{1}H-^{15}N HETCOR spectra from either the M2FL in DOPC/DOPE [14] or the truncated M2 protein in viral-envelope-mimetic lipid membranes [13] show correlations between water and the His_{37} imidazolium nitrogen, indicating that water molecules are involved in proton conductance. However, the HETCOR spectra represent only the equilibrium state in water-protein exchange processes at a given CP contact time during which complex exchange processes take place, therefore, their interpretation could yield different conductance mechanisms. On the other hand, the water-protein chemical exchange measurement sheds light onto the kinetic process of the water with hydronium ions interacting with the protons in the His_{37} tetrad, leading to a better understanding of the conductance mechanism of the M2 proton channel.

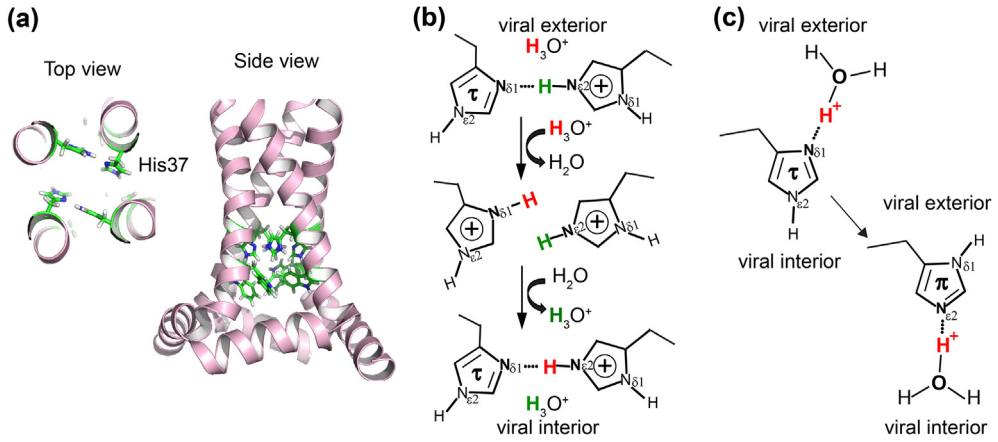

Fig. 5. (a) Conductance domain of the M2 proton channel from the Influenza A virus. (b) The low-barrier hydrogen bond model. The proton is transferred through the breaking and reforming of the intermonomer imidazole-imidazolium hydrogen bonds between the His_{37} residues. (c) The water-His_{37} hydrogen bonding model. The His_{37} shuttles protons through imidazole ring reorientations and exchanges protons with water. (b) and (c) were adapted with permission from Ref. [69] Copyright 2021 American Chemical Society.

Fig. 6a and b shows the expanded ^{15}N spectra of the His_{37}-labeled M2FL at different pHs in lipid bilayers using various t_{SL} values. The description of the M2FL samples and experimental details can be found in Supporting Information. Clearly, the ^{15}N spectra (black) without ^{15}N dephasing show similar line-shapes and intensities at different t_{SL}. With a short LGCP contact time, the ^{15}N signals were only cross-polarized from the protonated ^{15}N sites of His_{37} sidechains (i.e., the τ state $N^{\tau}_{\varepsilon 2}$ and the charged state $N^{+}_{\delta 1}$ and $N^{+}_{\varepsilon 2}$). The non-protonated τ state $N^{\tau}_{\delta 1}$ (~250 ppm) could hardly be polarized. These observed ^{15}N resonances are spread from 165 to ~200 ppm, while their correlated ^{1}H frequencies extend up to 19 ppm [14]. Such high ^{15}N and ^{1}H frequencies indicate the formation of short imidazole-imidazolium H-bonds [67]. When ^{15}N selective dephasing was applied, the bonded protons of the charged His_{37} H-$N^{+}_{\delta 1}$ and H-$N^{+}_{\varepsilon 2}$ sites were dephased at the beginning of LGSL, thus no signals from the charged His_{37} $N^{+}_{\delta 1}$ or $N^{+}_{\varepsilon 2}$ protons were expected. However, in the presence of the water-protein exchange, the proton from the charged His_{37} H-$N^{+}_{\delta 1}$ or H-$N^{+}_{\varepsilon 2}$ (presumably H-$N^{+}_{\varepsilon 2}$) was re-energized during LGCP, such that the signals from the charged His_{37} $N^{+}_{\delta 1}$ or $N^{+}_{\varepsilon 2}$ could still be observed. As shown in the red spectra, the ^{15}N signals were largely reduced at a short t_{SL} (50 or 100 μs). Clearly from Fig. 6a and b, much of the spectral intensity that appears at ~165 ppm in black was not recovered in the red spectra even when t_{SL} was long, indicating that these signals at ~165 ppm belong to $N^{\tau}_{\varepsilon 2}$ that is less accessible by the hydronium ions. This assignment was confirmed by the ^{15}N-^{15}N correlation spectrum [27]. It is clear from the red spectra of Fig. 6a and b that the dipolar-dephased ^{15}N signals from the charged His_{37} $N^{+}_{\delta 1}$ or $N^{+}_{\varepsilon 2}$ recovered their intensities as t_{SL} increased, implying that their bonded protons gain magnetization during LGSL. As ^{1}H spin diffusion is suppressed during the LGSL and any relayed transfer is largely eliminated (c.f. Fig. 4), this observed gain can only be facilitated by chemical exchange between this particular proton and the hydronium ions.

Fig. 6c and d shows the recovery of the dipolar-dephased ^{15}N signals as a function of t_{SL}. Clearly, the signal recovery at pH 5.8 is much faster, reaching the maximum at t_{SL} of ~ 0.5 ms, as opposed to that at t_{SL} of ~ 1.2 ms at pH 6.2. In separate experiments, $T^{H}_{1\rho}$ was measured to be 16.2 and 15.8 ms for pH 6.2 and 5.8, respectively. These values were used as a constant to fit the recovery trajectories, yielding the exchange rate constant K_{IM} of 1750 ± 550 s^{-1} and 4000 ± 1500 s^{-1} between hydronium ions and the protons in the His_{37} NH bonds for the M2FL for pH 6.2 and 5.8, respectively, at −10 °C. It appears that K_{IM} at pH 5.8 is about twice as fast as that at pH 6.2 [15], indicating that the increase of the proton dynamics at lower pH is directly proportional to the proton concentration. Again, this represents an average value over a number of different His_{37} states with various exposures to hydronium ions. It is anticipated that the exchange model [14,15] established at −10 °C should be relevant at the physiological temperature but the exchange rates should be faster.

Different from the HETCOR spectra that represent the equilibrium state in water-protein exchange processes and cannot be used to trace the origin of the water-protein cross peaks, the observed kinetic recovery of the dipolar-dephased ^{15}N signals supports the low-barrier hydrogen bond model and discriminates against the proton shuttling mechanism [12,13] in the M2FL proton channel in lipid bilayers. In the proton shuttling mechanism [12,13], the non-protonated ^{15}N site by accepting a proton from a hydronium ion originating from the viral exterior becomes protonated and thus is not capable of receiving an additional hydronium ion, as it has to remain facing the viral exterior so that the other ^{15}N site in the same His residue can be ready to release its proton to the viral interior. Furthermore, this proton transport seems to involve only the protonation of the neutral His_{37} residues followed by deprotonation of these residues. In other words, the protonated ^{15}N signals from the charged His_{37} residues should not regain any intensity when dephased, but the protonated ^{15}N signals from the neutral His_{37} residues are expected to recover fully. This is contrary to the kinetic recovery processes observed in Fig. 6c and d, where the protonated ^{15}N signals at ~175 ppm from the charged His_{37} sites almost recover to their full intensities and only a fraction of the signals at ~166 ppm (partly from the neutral His_{37} residues) have regained their intensity. On the other hand, this kinetic

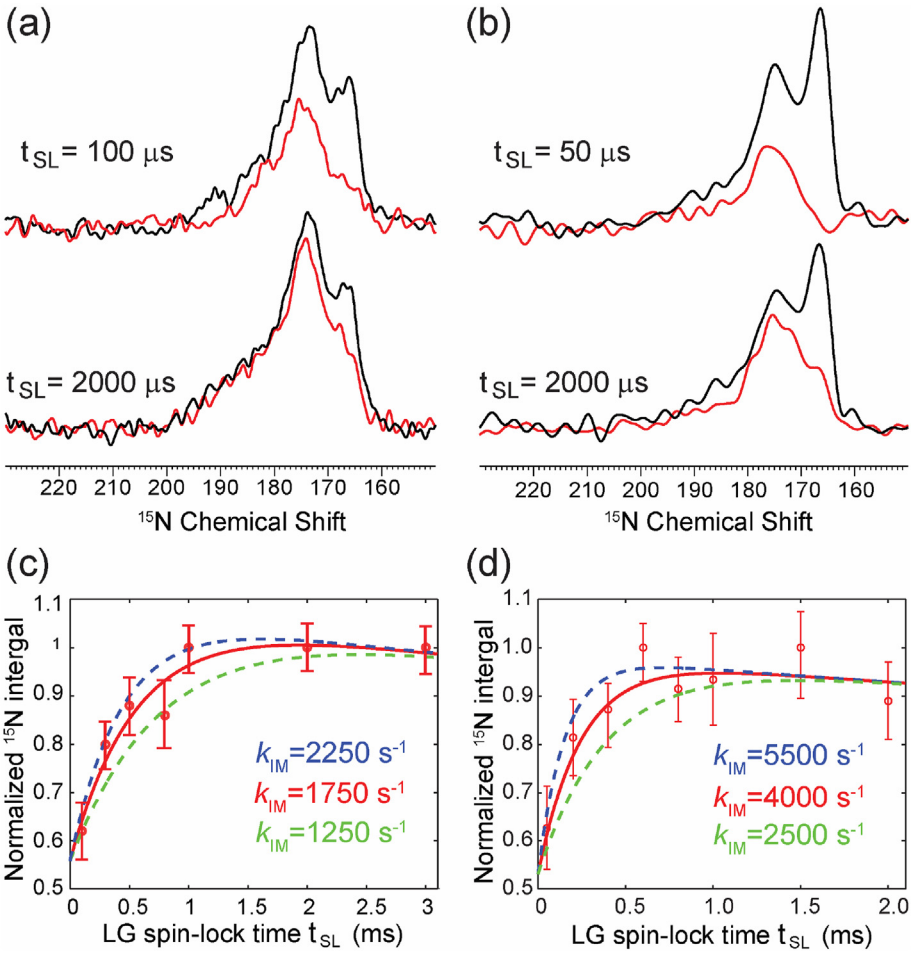

Fig. 6. (Top) Expanded ^{15}N MAS spectra of the His_{37}-labeled M2FL at pH 6.2 (a) and pH 5.8 (b) in lipid bilayers at −10 °C without (black) and with (red) ^{15}N-dipolar dephasing in different spinlock time t_{SL}. (Bottom) Normalized dipolar-dephased ^{15}N integral over the region of 200 and 160 ppm as a function of t_{SL} at pH 6.2 (c) and pH 5.8 (d). The red lines represent the best fit curves. Adapted with permission from Refs. [15] and [27]. Copyright 2021 American Chemical Society.

recovery can be well explained by the LBHB model: 1) the reformed imidazole-imidazolium hydrogen bonding His_{37} pairs always allow the His_{37} tetrad to be ready for accepting the next hydronium ion. 2) In the His_{37} tetrad, as illustrated in Fig. 5b, all of the green protons are dephased in applying the ^{15}N REDOR dephasing sequence. But the red protons from water are taking the green proton positions through the exchange processes allowing the recovery of the dipolar-dephased ^{15}N signals. The existence of such intermonomer imidazole-imidazolium hydrogen bonds has evidently been confirmed by the observation of the hydrogen-bond mediated ^{15}N-^{15}N *J*-couplings [68,69].

Similarly, converting this 1D version of the chemical exchange measurements diagramed in Fig. 3a into a 2D version would allow for site-specific determinations of water accessibility, as demonstrated in the Aquaporin Z membrane protein [70].

5. Conclusions and perspectives of water-protein chemical exchange experiments in solid-state NMR

It is known that coherent SD and incoherent chemical exchange as well as NOE are classified as water-protein polarization transfer mechanisms [25,30,31]. These mechanisms represent different water-protein interactions: SD is distance-dependent, mediated by intermolecular ^{1}H-^{1}H dipolar interactions, and therefore can reveal the specific sites in the protein that bonds with water. Although the intramolecular dipolar couplings in the protein do not directly contribute to the water-protein polarization transfer, they can rapidly disperse the water-protein transferred polarization into other protons in the protein obscuring the detection of the site-specific water-protein transfer. Chemical exchange is the proton substitution process between the proton in water molecules and protons in the protein, and thus provides an important tool for characterizing the role of water in the structure and function of the protein. While NOE is based on dipolar cross effects between two motional-modulated spins that are in close proximity, and thus can be used to enhance specific ^{15}N/^{13}C sites in the protein that are in the water-protein interface [30,71–73]. However, ^{1}H-^{1}H NOE between water and protein protons is dominated by long-range

dipolar couplings to bulk water [48]. Temperature is an important variable to control the water-protein polarization transfer contributions from various mechanisms, as it is sensitive to the incoherent chemical exchange/NOE. On the other hand, fast MAS has been used to probe the structured water that contributes to the polymorphic nature of pharmaceuticals [74]. It could dramatically weaken the ^{1}H homonuclear dipolar interactions and thus suppress the SD, making the chemical exchange and/or NOE contributions dominant. Therefore, differentiating the underlying water-protein polarization transfer mechanisms is important in terms of knowing exactly how water interacts with the protein. In particular, the chemical exchange mechanism provides a unique opportunity to understand how water participates in the structure and function of the protein. As demonstrated above with the example of the M2FL protein, the measurements of the kinetic processes of the pure chemical exchange between water and the protons in the His_{37} NH bonds in the center of the M2FL transmembrane helix allow for the characterization of the proton conduction mechanism in the M2 proton channel.

Another perspective for pure water-protein chemical exchange experiments is to utilize the mobile water for detecting those invisible or buried protons that are in exchange with water in membrane-bound proteins/peptides. It is well known that by saturating a small proton resonance via continuous irradiation, the large unsaturated proton magnetization (i.e., water ^{1}H signal) continuously moves to the saturated proton resonance through chemical exchange, a process called chemical exchange saturation transfer (CEST) [75]. Consequently, the water signal decreases and therefore, by directly monitoring the sensitive water signal, those proton sites in exchange with water can be revealed, even though they are severely overlapped by other ^{1}H resonances. The CEST method has been exclusively used in solution NMR for studying protein folding [76–81] and it has recently been extended to a static ^{2}H application in biological solids [82], but it has yet to be utilized in solid-state NMR of membrane-bound proteins/peptides due to the strong ^{1}H-^{1}H spin diffusion in the relatively rigid membrane bound proteins. With the suppression of ^{1}H-^{1}H spin diffusion either by spin-locking along the MA or by fast MAS, the CEST experiments become possible in the study of membrane bound proteins/peptides.

Fig. 7 shows the potential of the CEST method (see Supporting Information) with gramicidin A (gA) samples hydrated in lipid bilayers for the first time, where the water relative signal intensity is plotted as a function of ^{1}H saturation offset, $\Delta\nu$. GA, an antibiotic from *Bacillus brevis*, is a polypeptide of 15 amino acid residues having the sequence of formyl-L-Val_1-Gly_2-L-Ala_3-D-Leu_4-L-Ala_5-D-Val_6-L-Val_7-D-Val_8-L-Trp_9-D-Leu_{10}-L-Trp_{11}-D-Leu_{12}-LTrp_{13}-D-Leu_{14}-L-Trp_{15}-ethanolamine. All the alternating D- and L-amino acid side chains project on one side of the β-strand secondary structure, so as to force the strand to take on a helical conformation. In lipid bilayers, the polypeptide forms a monovalent cation selective channel that is dimeric, but single-stranded. The high-resolution structure of the channel monomer has been defined with 120 precise orientational constraints from solid-state NMR of uniformly aligned samples in lipid [83–85]. The polypeptide backbone lines the pore wide enough only for a single file of water molecules. For monovalent cations to pass through the pore, they must be stripped of all but two of their waters of solvation prior to entering the single file region of the pore. In Fig. 7, no water ^{1}H signal can be observed when the ^{1}H saturation is applied to the water resonance itself at 4.7 ppm, but its signal intensity is not affected as the ^{1}H saturation offset moves away, unless the saturation offset is close to ^{1}H sites that are in exchange with water. Clearly, the CEST profiles indicate a significant signal at ~7.7 ppm, suggesting the existence of a ^{1}H site in the gA channel that chemically exchanges with water on the time scale of milliseconds which is consistent with the recent ^{17}O study indicating great stability for the N-H ... *O*═C hydrogen bonds [34]. Since the mobile water molecules themselves are generating high

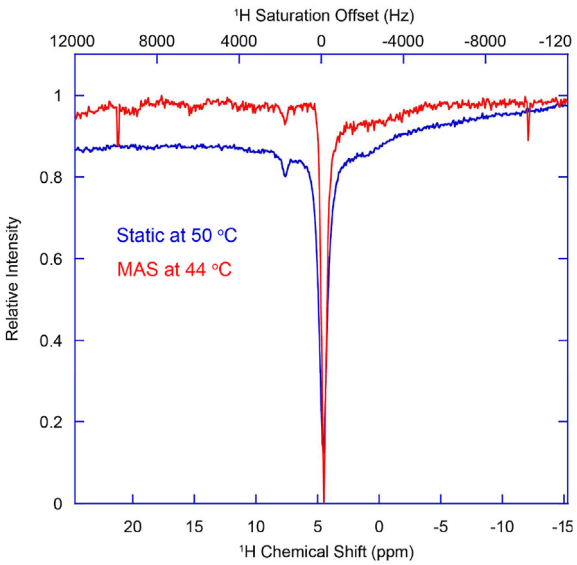

Fig. 7. Plots of water ^{1}H signal intensity as a function of ^{1}H saturation offset recorded on 600 MHz for the gramicidin A sample hydrated in lipids under static (blue) and 10 kHz MAS (red) conditions.

resolution resonances without the need of fast MAS, the CEST experiments can also be applied in the static or mechanically aligned gA sample, as shown in the blue curve in Fig. 7. It is noted that the dips at ± 10 kHz are also observed in the CEST profile representing the rotary resonance condition under MAS [41,86]. Moreover, the residual quadrupolar couplings of water were observed in ^{17}O NMR spectra, indicating the water dynamics in the interface of lipid bilayers [34] as well as in polymer-based lipid-nanodiscs [87].

It is worth noting that, for CEST experiments, slow to intermediate exchange conditions on the NMR time scale must be fulfilled, i.e., $\Delta\nu_{IM} >> K_{IM}$ or $\Delta\nu_{IM} \sim K_{IM}$, where $\Delta\nu_{IM}$ (in Hz) is the chemical shift difference between water and a specific proton site with an exchange rate of K_{IM}. Therefore, ultra-high fields [88] have a great advantage for CEST experiments as $\Delta\nu_{IM}$ increases, expanding measurable K_{IM} values that cannot be observed at lower fields. Since water is critical for the functioning of membrane-bound proteins/peptides [89–91] and chemical exchange is an extremely common phenomenon in protein science, it is anticipated that the pure water-protein chemical exchange experiments in biological solids would provide a new opportunity to characterize structure-function relationships of membrane bound proteins/peptides.

Declaration of competing interest

The authors declare no competing financial interest.

Acknowledgement

This work was supported by NIH Grants AI023007 and GM122698. All NMR experiments were carried out at the National High Magnetic Field Lab (NHMFL) supported by the NSF Cooperative Agreement DMR-1644779 and the State of Florida.

Appendix A. Supplementary data

Supplementary data to this article can be found online at https://doi.org/10.1016/j.mrl.2021.09.002.

References

[1] A.D. Dupuy, D.M. Engelman, Protein area occupancy at the center of the red blood cell membrane, Proc. Natl. Acad. Sci. U.S.A. 105 (2008) 2848–2852.
[2] H.T. McMahon, J.L. Gallop, Membrane curvature and mechanisms of dynamic cell membrane remodelling, Nature 438 (2005) 590–596.
[3] J.T. Groves, J. Kuriyan, Molecular mechanisms in signal transduction at the membrane, Nat. Struct. Mol. Biol. 17 (2010) 659–665.
[4] M. Schmick, P.I.H. Bastiaens, The interdependence of membrane shape and cellular signal processing, Cell 156 (2014) 1132–1138.
[5] M.F. Brown, Modulation of rhodopsin function by properties of the membrane lilayer, Chem. Phys. Lipids 73 (1994) 159–180.
[6] M.D. C, S.L. Niu, B.J. Litman, Enhancement of G protein-coupled signaling by DHA phospholipids, Lipids 38 (2003) 437–443.
[7] O. Soubias, K. Gawrisch, The role of the lipid matrix for structure and function of the GPCR rhodopsin, Biochim. Biophys. Acta 1818 (2012) 234–240.
[8] H.X. Zhou, T.A. Cross, Influences of membrane mimetic environments on membrane protein structures, Annu. Rev. Biophys. 42 (2013) 361–392.
[9] T.A. Cross, D.T. Murray, A. Watts, Helical membrane protein conformations and their environment, Eur. Biophys. J. 42 (2013) 731–755.
[10] J. Hu, R. Fu, K. Nishimura, L. Zhang, H.X. Zhou, D.D. Busath, V. Vijayvergiya, T.A. Cross, Histidines, heart of the hydrogen ion channel from influenza A virus: toward an understanding of conductance and proton selectivity, Proc. Natl. Acad. Sci. U.S.A. 103 (2006) 6865–6870.
[11] R. Fu, E.D. Gordon, D.J. Hibbard, M. Cotten, High resolution heteronuclear correlation NMR spectroscopy of an anitimicrobial peptide in aligned lipid bilayers: peptide-water interactions at the water-bilayer interface, J. Am. Chem. Soc. 131 (2009) 10830–10831.
[12] F. Hu, K. Schmidt-Rohr, M. Hong, NMR detection of pH-dependent histidine-water proton exchange reveals the conduction mechanism of a transmembrane proton channel, J. Am. Chem. Soc. 134 (2012) 3703–3713.
[13] M. Hong, K.J. Fritzsching, J.K. William, Hydrogen-bonding partner of the proton-conducting histidine in the influenza M2 proton channel revealed from ^{1}H chemical shifts, J. Am. Chem. Soc. 134 (2012) 14753–14755.
[14] Y. Miao, R. Fu, H.X. Zhou, T.A. Cross, Dynamic short hydrogen bonds in histidine tetrad of full length M2 proton channel reveal tetrameric structural heterogeneity and functional mechanism, Structure 23 (2015) 2300–2308.
[15] R. Fu, Y. Miao, H. Qin, T.A. Cross, Probing hydronium ion histidine NH exchange rate constants in the M2 channel via indirect observation of dipolar-dephased ^{15}N signals in solid-state magic-angle-spinning NMR, J. Am. Chem. Soc. 138 (2016) 15801–15804.
[16] R.G. Bryant, The dynamics of water-protein interactions, Annu. Rev. Biophys. Biomol. Struct. 25 (1996) 29–53.
[17] N.V. Nucci, M.X. Pometun, A.J. Wand, Site-resolved measurement of water-protein interactions by solution NMR, Nat. Struct. Mol. Biol. 18 (2011) 245–250.
[18] S. Martini, C. Bonechi, A. Foletti, C. Rossi, Water-protein interactions: the secret of protein dynamics, Sci. World J. 2013 (2013), 1138916.
[19] O. Otting, E. Liepinsh, K. Wuthrich, Protein hydration in aqueous solution, Science 254 (1991) 974–980.
[20] D. Huster, Y. Yao, M. Hong, Membrane protein topology probed by ^{1}H spin diffusion from lipids using solid-state NMR spectroscopy, J. Am. Chem. Soc. 124 (2002) 874–883.
[21] A. Bockmann, M. Juy, E. Bettler, L. Emsley, A. Galinier, F. Penin, A. Lesage, Water-protein hydrogen exchange in the micro-crystalline protein Crh as observed by solid state NMR spectroscopy, J. Biomol. NMR 32 (2005) 195–207.
[22] C. Ader, R. Schneider, K. Seidel, M. Etzkorn, S. Becker, M. Baldus, Structural rearrangements of membrane proteins probed by water-edited solid-state NMR spectroscopy, J. Am. Chem. Soc. 131 (2009) 170–176.
[23] V. Chevelkov, S.Q. Xiang, K. Giller, S. Becker, A. Lange, B. Reif, Perspectives for sensitivity enhancement in proton-detected solid-state NMR of highly deuterated proteins by preserving water magnetization, J. Biomol. NMR 61 (2015) 151–160.
[24] S.H. Li, Y.C. Su, W.B. Luo, M. Hong, Water-protein interactions of an arginine-rich membrane peptide in lipid bilayers investigated by solid-state nuclear magnetic resonance spectroscopy, J. Phys. Chem. B 114 (2010) 4063–4069.
[25] J.K. William, M. Hong, Probing membrane protein structure using water polarization transfer solid-state NMR, J. Magn. Reson. 247 (2014) 118–127.
[26] J.K. William, D. Tietze, M. Lee, J. Wang, M. Hong, Solid-state NMR investigation of the conformation, proton conduction, and hydration of the influenza B virus M2 transmembrane proton channel, J. Am. Chem. Soc. 138 (2016) 8143–8155.
[27] H. Qin, Y. Miao, T.A. Cross, R. Fu, Beyond structural biology to functional biology: solid-state NMR experiments and strategies for understanding the M2 proton channel conductance, J. Phys. Chem. B 121 (2017) 4799–4809.

[28] H. Singh, S.K. Vasa, H. Jangra, P. Rovo, C. Paslack, C.K. Das, H. Zipse, L.V. Schaefer, R. Linser, Fast microsecond dynamics of the protein-water network in active site of human carbonic anhydrase II studied by solid-state NMR spectroscopy, J. Am. Chem. Soc. 141 (2019) 19276–19288.
[29] A. Dicke, T. Gopinath, Y. Wang, G. Veglia, Probing residue-specific water-protein interactions in oriented lipid membranes via solid-state NMR spectroscopy, J. Phys. Chem. B 120 (2016) 10959–10968.
[30] A. Lesage, L. Emsley, F. Penin, A. Bockmann, Investigation of dipolar-mediated water-protein interactions in microcrystalline Crh by solid-state NMR spectroscopy, J. Am. Chem. Soc. 128 (2006) 8246–8255.
[31] A. Lesage, A. Bockmann, Water-protein interactions in microcrystalline Crh measured by H-1-C-13 solid-state NMR spectroscopy, J. Am. Chem. Soc. 125 (2003) 13336–13337.
[32] C.L. Tian, P.F. Gao, L.H. Pinto, R.A. Lamb, T.A. Cross, Initial structural and dynamic characterization of the M2 protein transmembrane and amphipathic helices in lipid bilayers, Protein Sci. 12 (2003) 2597–2605.
[33] S. Wang, L. Shi, I. Kawamura, L.S. Brown, V. Ladizhansky, Site-specific solid-state NMR detection of hydrogen-deuterium exchange reveals conformational changes in a 7-helical transmembrane protein, Biophys. J. 101 (2011) L23–L25.
[34] J. Paulino, M. Yi, I. Hung, Z. Gan, X. Wang, E.Y. Chekmenev, H.X. Zhou, T.A. Cross, Functional stability of water wire-carbonyl interactions in an ion channel, Proc. Natl. Acad. Sci. U.S.A 117 (2020) 11908–11915.
[35] H. Shen, Z. Wu, X. Zou, Interfacial water structure at zwitterionic membrane/water interface: the importance of interactions between water and lipid carbonyl groups, ACS Omega 5 (2020) 18080–18090.
[36] E.A. Disalvo, F. Lairion, F. Martini, E. Tymczyszyn, M. Frias, H. Almaleck, G.J. Gordillo, Structural and functional properties of hydration and confined water in membrane interfaces, Biochim. Biophys. Acta 1778 (2008) 2655–2670.
[37] A.C. Fogarty, D. Laage, Water dynamics in protein hydration shells: the molecular origins of the dynamical perturbation, J. Phys. Chem. B 118 (2014) 7715–7729.
[38] G.S. Harbison, J.E. Roberts, J. Herzfeld, R.G. Griffin, Solid-state NMR detection of proton exchange between the bacteriorhodopsin Schiff base and bulk water, J. Am. Chem. Soc. 110 (1988) 7221–7223.
[39] M. Lee, W. Goldburg, Nuclear magnetic resonance line narrowing by a rotating RF field, Phys. Rev. 140 (1965) 1261–1271.
[40] D. Canet, H. Python, D. Grandclause, P. Mutzenhardt, Analytical solution to Solomon equations for three-spin groupings, J. Magn. Reson., Ser. A 122 (1996) 204–208.
[41] K. Takegoshi, S. Nakamura, T. Terao, C-13-H-1 dipolar-assisted rotational resonance in magic-angle spinning NMR, Chem. Phys. Lett. 344 (2001) 631–637.
[42] M. Weingarth, D.E. Demco, G. Bodenhausen, P. Tekely, Improved magnetization transfer in solid-state NMR with fast magic angle spinning, Chem. Phys. Lett. 469 (2009) 342–348.
[43] Y.F. Wei, A. Ramamoorthy, 2D ^{15}N-^{15}N isotropic chemical shift correlation established by ^{1}H-^{1}H dipolar coherence transfer in biological solids, Chem. Phys. Lett. 342 (2001) 312–316.
[44] A.E. Bennett, R.G. Griffin, J.H. Ok, S. Vega, Chemical shift correlation spectroscopy in rotating solids: radio frequency-driven dipolar recoupling and longitudinal exchange, J. Chem. Phys. 96 (1992) 8624–8627.
[45] A. Ramamoorthy, J. Xu, 2D ^{1}H/^{1}H RFDR and NOESY NMR experiments on a membrane-bound antimicrobial peptide under magic angle spinning, J. Phys. Chem. B 117 (2013) 6693–6700.
[46] M.K. Pandey, S. Vivekanandan, K. Yamamoto, S. Im, L. Waskell, A. Ramamoorthy, Proton-detected 2D radio frequency driven recoupling solid-state NMR studies on micelle-associated cytochrome-b_5, J. Magn. Reson. 242 (2014) 169–179.
[47] S.A. Kotler, J.R. Brender, S. Vivekanandan, Y. Suzuki, K. Yamamoto, M. Monette, J. Krishnamoorthy, P. Walsh, M. Cauble, M.M.B. Holl, E.N.G. Marsh, A. Ramamoorthy, High-resolution NMR characterization of low abundance oligomers of amyloid-β without purification, Sci. Rep. 5 (2015), 11811.
[48] K. Modig, E. Liepinsh, O. Otting, B. Halle, Dynamics of protein and peptide hydration, J. Am. Chem. Soc. 126 (2004) 102–114.
[49] J.P. Demers, V. Chevelkov, A. Lange, Progress in correlation spectroscopy at ultra-fast magic-angle spinning: basic building blocks and complex experiments for the study of protein structure and dynamics, Solid State Nucl. Magn. Reson. 40 (2011) 101–113.
[50] M. Deschamps, Ultrafast magic angle spinning nuclear magnetic resonance, Annu. Rep. NMR Spectrosc. 81 (2014) 109–144.
[51] I.V. Sergeyev, S. Bahri, L.A. Day, A.E. McDermott, Pf1 bacteriophage hydration by magic angle spinning solid-state NMR, J. Chem. Phys. 141 (2014), 22D533.
[52] Y. Miao, T.A. Cross, R. Fu, Differentiation of histidine tautomeric states using ^{15}N selectively filtered ^{13}C solid-state NMR spectroscopy, J. Magn. Reson. 245 (2014) 105–109.
[53] Y. Pan, T. Gullion, J. Schaefer, Determination of C-N internuclear distances by rotational-echo double-resonance NMR of solids, J. Magn. Reson. 90 (1990) 330.
[54] R.J. Sugrue, A.J. Hay, Structural characteristics of the M2 protein of influenza-A viruses - evidence that it forms a tetrameric channel, Virology 180 (1991) 617–624.
[55] T. Sakaguchi, Q.A. Tu, L.H. Pinto, R.A. Lamb, The active oligomeric state of the minimalistic influenza virus M-2 ion channel is a tetramer, Proc. Natl. Acad. Sci. U.S.A. 94 (1997) 5000–5005.
[56] J. Hu, T. Asbury, S. Achuthan, C. Li, R. Bertram, J.R. Quine, R. Fu, T.A. Cross, Backbone structure of the amantadine-blocked trans-membrane domain M2 proton channel from influenza A virus, Biophys. J. 92 (2007) 4335–4343.
[57] K. Nishimura, S.G. Kim, L. Zhang, T.A. Cross, The closed state of a H+ channel helical bundle combining precise orientational and distance restraints from solid state NMR, Biochemistry 41 (2002) 13170–13177.
[58] R.A. Lamb, S.L. Zebedee, C.D. Richardson, Influenza virus-M2 protein is an integral membrane-protein expressed on the infected-cell surface, Cell 40 (1985) 627–633.
[59] S. Grambas, M.S. Bennett, A.J. Hay, Influence of amantadine resistance mutations on the pH regulatory function of the M2-protein of influenza-A viruses, Virology 191 (1992) 541–549.
[60] M. Sharma, M. Yi, H. Dong, H. Qin, E. Peterson, D.D. Busath, H.X. Zhou, T.A. Cross, Insight into the mechanism of the influenza A proton channel from a structure in a lipid bilayer, Science 330 (2010) 509–512.
[61] T.V. Can, M. Sharma, I. Hung, P.L. Gor'kov, W.W. Brey, T.A. Cross, Magic angle spinning and oriented sample solid-state NMR structural restraints combine for influenza A M2 protein functional insights, J. Am. Chem. Soc. 134 (2012) 9022–9025.
[62] L.B. Andreas, M.T. Eddy, R.M. Pielak, J.J. Chou, R.G. Griffin, Magic angle spinning NMR investigation of Influenza A $M2_{18-60}$: support for an allosteric mechanism of inhibition, J. Am. Chem. Soc. 132 (2010) 10958–10960.
[63] L.B. Andreas, M.T. Eddy, J.J. Chou, R.G. Griffin, Magic-angle-spinning NMR of the drug resistant S31N M2 proton transporter from Influenza A, J. Am. Chem. Soc. 134 (2012) 7215–7218.
[64] M.T. Colvin, L.B. Andreas, J.J. Chou, R.G. Griffin, Proton association constants of His 37 in the Influenza-A M218-60 dimer-of-dimers, Biochemistry 53 (2014) 5987–5994.
[65] L.B. Andreas, M. Reese, M.T. Eddy, V. Gelev, Q.Z. Ni, E.A. Miller, L. Emsley, G. Pintacuda, J.J. Chou, R.G. Griffin, Structure and mechanism of the influenza A m218-60 dimer of dimers, J. Am. Chem. Soc. 137 (2015) 14877–14886.
[66] Y. Miao, H. Qin, R. Fu, M. Sharma, T.V. Can, I. Hung, S. Luca, P.L. Gor'kov, W.W. Brey, T.A. Cross, M2 proton channel structural validation from full-length protein samples in synthetic bilayers and *E. coli* membranes, Angew. Chem. 124 (2012) 8508–8511.
[67] H. Eckert, J.P. Yesinowski, L.A. Silver, E.M. Stolper, Water in silicate glasses: quantitation and structural studies by proton solid echo and magic angle spinning NMR methods, J. Phys. Chem. 92 (1988) 2055–2064.
[68] C.H. Tan, Y. Chen, X. Peng, Z. Chen, S.H. Cai, T.A. Cross, R. Fu, Revealing weak histidine ^{15}N homonuclear scalar couplings using solid-state magic-angle-spinning NMR spectroscopy, J. Magn. Reson. 316 (2020), 106757.

[69] R. Fu, Y. Miao, H. Qin, T.A. Cross, Observation of the imidazole-imidazolium hydrogen bonds responsible for selective proton conductance in the influenza A M2 channel, J. Am. Chem. Soc. 142 (2020) 2115–2119.
[70] Y.X. Zhao, H.Y. Xie, L. Wang, Y. Shen, W. Chen, B.T. Song, Z. Zhang, A. Zheng, Q. Lin, R. Fu, J. Wang, J. Yang, Gating mechanism of Aquaporin Z in synthetic bilayers and native membranes revealed by solid-state NMR spectroscopy, J. Am. Chem. Soc. 140 (2018) 7885–7895.
[71] K. Takegoshi, T. Terao, C-13 nuclear Overhauser polarization nuclear magnetic resonance in rotating solids: replacement of cross polarization in uniformly C-13 labeled molecules with methyl groups, J. Chem. Phys. 117 (2002) 1700–1707.
[72] J.Y. Cui, J. Li, X. Peng, R. Fu, Transient NOE enhancement in solid-state MAS NMR of mobile systems, J. Magn. Reson. 284 (2017) 73–79.
[73] R. Zhang, K.H. Mroue, A. Ramamoorthy, Hydridizing cross-polarization with NOE or refocused-INEPT enhances the sensitivity of MAS NMR spectroscopy, J. Magn. Reson. 266 (2016) 59–66.
[74] J.T. Damron, K.M. Kersten, M.K. Pandey, Y. Nishiyama, A. Matzger, A. Ramamoorthy, Role of anomalous water constraints in the efficacy of pharmaceuticals probed by 1H solid-state NMR, ChemistrySelect 2 (2017) 6797–6800.
[75] J.Y. Zhou, P.C.M. van Zijl, Chemical exchange saturation transfer imaging and spectroscopy, Prog. Nucl. Magn. Reson. Spectrosc. 48 (2006) 109–136.
[76] T. Yuwen, A. Sekhar, L.E. Kay, Separating dipolar and chemical exchange magnetization transfer processes in ^{1}H-CEST, Angew. Chem. 56 (2016) 6122–6125.
[77] P. Vallurupalli, A. Sekhar, T. Yuwen, L.E. Kay, Probing conformational dynamics in biomolecules via chemical exchange saturation transfer: a primer, J. Biomol. NMR 67 (2017) 243–271.
[78] T. Yuwen, R. Huang, L.E. Kay, Probing slow timescale dynamics in proteins using methyl ^{1}H CEST, J. Biomol. NMR 68 (2017) 215–224.
[79] T. Yuwen, L.E. Kay, Longitudinal relaxation optimized amide ^{1}H-CEST experiments for studying slow chemical exchange processes in fully protonated proteins, J. Biomol. NMR 67 (2017) 295–307.
[80] T. Yuwen, L.E. Kay, A new class of CEST experiment based on selecting different magnetization components at the start and end of the CEST relaxation element: an application to ^{1}H CEST, J. Biomol. NMR 70 (2018) 93–102.
[81] V. Tugarinov, G.M. Clore, Exchange saturation transfer and associated NMR techniques for studies of protein interactions involving high-molecular-weight systems, J. Biomol. NMR 73 (2019) 461–469.
[82] L. Vugmeyster, D. Ostrovsky, R. Fu, Deuteron quadrupolar chemical exchange saturation transfer (Q-CEST) solid-state NMR for static powder samples: approach and applications to amyloid-β fibrils, ChemPhysChem 21 (2020) 220–231.
[83] R. Ketchem, W. Hu, T.A. Cross, High-resolution conformation of gramicidin A in a lipid bilayer by solid-state NMR, Science 261 (1993) 1457–1460.
[84] R. Ketchem, B. Boux, T.A. Cross, High-resolution polypeptide structure in a lamellar phase lipid environment from solid state NMR derived orientational constraints, Structure 5 (1997) 1655–1669.
[85] F. Kovacs, J.R. Quine, T.A. Cross, Validation of the single-stranded channel conformation of gramicidin A by solid-state NMR, Proc. Natl. Acad. Sci. U.S.A 96 (1999) 7910–7915.
[86] T.G. Oas, R.G. Griffin, M.H. Levitt, Rotary resonance recoupling of dipolar interactions in solid-state nuclear magnetic resonance spectroscopy, J. Chem. Phys. 89 (1988) 692–695.
[87] T. Ravula, B.R. Sahoo, X. Dai, A. Ramamoorthy, Natural-abundance ^{17}O NMR spectroscopy of magnetically aligned lipid nanodiscs, Chem. Commun. 56 (2020) 9998–10001.
[88] Z. Gan, I. Hung, X. Wang, J. Paulino, G. Wu, I.M. Litvak, P. Gor'kov, W.W. Brey, P. Lendi, J.L. Schiano, M.D. Bird, I.R. Dixin, J. Toth, G.S. Boebinger, T.A. Cross, NMR spectroscopy up to 35.2 T using a series-connected hybrid magnet, J. Magn. Reson. 284 (2017) 125–136.
[89] L.C. Nabwetter, M. Fischer, H.A. Scheidt, H. Heerklotz, Membrane-water partitioning – tackling the challenges of poorly soluble drugs using chaotropic co-solvents, Biophys. Chem. 277 (2021), 106654.
[90] H. Hadidi, R. Kamali, Molecular dynamics study of water transport through AQP5-R188C mutant causing palmoplantar keratoderma (PPK) using the gating, Biophys. Chem. 277 (2021), 106655.
[91] M. Goto, A. Kazama, K. Fukuhara, H. Sato, N. Tamai, H.O. Ito, H. Matsuki, Membrane fusion of phospholipid bilayers under high pressure: spherical and irreversible growth of giant vesicles, Biophys. Chem. 277 (2021), 106639.

Rongfu Zhang received the B.S. degree in ecology and M.S. degree in biochemistry from the School of Life Science, Xiamen University in 2007 and 2010 respectively. He received his PhD degree in biochemistry from the Chemistry and Biochemistry department, Miami University in 2016. Currently, he is a postdoc at National High Magnetic Field Laboratory located at Tallahassee, Florida. His research interests include membrane protein structural characterizations using ssNMR and EPR spectroscopies.

Timothy A. Cross received his B.S. degree in Chemistry from Trinity College, Hartford, CT, USA in 1976 and his PhD in 1981 with Stanley J. Opella at the University of Pennsylvania. Following a short postdoctoral fellowship with Opella, he had a second postdoc with Joachim Seelig at the Biozentrum in Basel, Switzerland before accepting a faculty position at Florida State University in 1984. In 1990 the National High Magnetic Field Lab was moved to FSU where he led the development of the NMR/MRI User Program. His research interests are in the structural and dynamic characterization of membrane peptides and proteins using solid state NMR spectroscopy.

Riqiang Fu received his B.S. degree in Electrical Engineering from University of Science and Technology (USTC) of China in 1986 and his PhD degree in 1992 with Prof. Chaohui Ye at Wuhan Institute of Physics. Currently he is a Research Faculty III at National High Magnetic Field Lab. He specializes in solid-state NMR methodology development and NMR applications in materials science (such as lithium ion battery materials) and biological systems (such as membrane proteins).

Rongfu Zhang, Timothy A. Cross
National High Magnetic Field Laboratory, 1800 East Paul Dirac Drive, Tallahassee, FL, 32310, USA

Department of Chemistry and Biochemistry, Florida State University, Tallahassee, FL, 32301, USA

Riqiang Fu*
National High Magnetic Field Laboratory, 1800 East Paul Dirac Drive, Tallahassee, FL, 32310, USA
* Corresponding author. National High Magnetic Field Laboratory, 1800 East Paul Dirac Drive, Tallahassee, FL, 32310, USA
E-mail address: rfu@magnet.fsu.edu

7 June 2021
Available online 30 November 2021